

A study of corrosion related electromagnetic signatures of marine vessels using a BEM.

P. Allan and A. Watt

*Department of Physics and Astronomy, Glasgow University,
Scotland.*

Abstract

Modelling the corrosion of marine vessels is a semi-infinite domain problem, with a large continuous volume. The BEM is the most suitable numerical method for calculating the electric potential and its normal derivative on the boundary from Laplace's Equation. With these known, it is possible to calculate the electric and magnetic fields due to corrosion, providing an insight into the level of corrosion protection provided and the detectability of the vessel to underwater threats. An innovative method has been developed for integrating the fundamental solution using triangular elements. This consists of performing the integrals by forming polynomials in which the variables are the moments of the element. By extracting the dimensions from the calculations of the moments, they can be calculated using normalised moments which depend solely on a 'shape' parameter. These normalised moments may be expressed as polynomials in this shape parameter where the coefficients are independent of the size or shape of the element. These coefficients can be calculated once and then referred to when required. Hence the integrals can be evaluated by forming polynomials where the coefficients are pre-calculated and the variable is a simple shape parameter. By limiting the polynomials to the order of twenty, the integral calculations have been shown to be accurate to six decimal places. This method has been used to model a ship of 50,000 tonne displacement. The resulting BEM equations are solved using a point successive over-relaxation method and calculations have been performed to investigate the convergence of this algorithm. Emphasis on realistic polarisation data and comparison to experimental data is subject to further development.

Keywords: boundary element, electromagnetic signatures, corrosion, triangular elements, magnetic field, point successive over-relaxation method.

1 Introduction

The electromagnetic signatures of marine vessels due to corrosion is important for detection and identification purposes (Jeffery & Brooking [1]). Corrosion currents in the sea around the vessel give rise to characteristic electric and magnetic fields. This paper considers how information on the electrochemical potentials at the interface between the hull and seawater, initially modified by protective coatings, may be used to calculate an electric potential around the vessel. As seawater is conducting, currents flow in the water and magnetic fields result. Both static and low frequency fields are present, but we confine ourselves to static fields. Although this problem has already been studied in the literature (Zamani & Porter [2], Wang *et al.* [3]) we believe that the methods used may be improved upon.

We assume the sea is represented by a finite rectangular box filled with homogeneous seawater, with the ship floating centrally on the top surface. The problem of electric fields in the box may be addressed by several methods, but we choose the Boundary Element Method (BEM) as the water is homogeneous. The "boundary" in this case is the bottom of the box, its front, rear, left and right faces, the surface of the submerged part of the hull and propeller, and that part of the surface of the sea on the top face outside the vessel. The boundary is then covered with discrete elements which we choose to be triangles. The nodes in the problem are taken to be the centroids of the triangles, and the electric potential over a triangle is assumed to be the same as its value at its centroid.

2 Implementation Summary of the BEM.

The derivation of the form of the BEM considered in this work can be found in Brebbia [4]. The basic equation describing the model is

$$H\mathbf{u} = G\mathbf{q} \quad (2.1)$$

where, for this model of a ship corroding in seawater, \mathbf{u} is a vector of the potentials on each element, and \mathbf{q} is the negative of the outward normal component of electric field emitted from each element. The values of the matrix coefficients are given by

$$H_{i,j} = \begin{cases} \frac{1}{4\pi} \int_{\Gamma_j} \frac{\partial}{\partial \mathbf{n}} \left(\frac{1}{R_{i,j}} \right) d\Gamma, & \text{when } i \neq j, \\ \frac{1}{4\pi} \int_{\Gamma_j} \frac{\partial}{\partial \mathbf{n}} \left(\frac{1}{R_{i,j}} \right) d\Gamma + \frac{1}{2}, & \text{when } i = j \end{cases} \quad (2.2)$$

$$G_{i,j} = \frac{1}{4\pi} \int_{\Gamma_j} \frac{1}{R_{i,j}} d\Gamma_j, \quad \forall i, j \quad (2.3)$$

where Γ_j is the surface of triangle j and \mathbf{n} is the outward normal to Γ_j . These come from the fundamental solution of Laplace's Equation in three-dimensions being (Brebbia [4])

$$\frac{1}{4\pi R_{i,j}} \quad (2.4)$$

Here the 'i' subscript refers to the source element whilst the 'j' subscript indicates the element over which the integral is performed.

Therefore to form the BEM equation, eqn (2.1), which describes the model, it is first necessary to calculate the coefficient matrices using these integrals.

As mentioned above, the elements of the mesh are chosen to be constant, and further they are chosen to be triangular as this geometry is simple and provides the ability to mesh complex surfaces (Zamani & Porter [2]). There exist many methods for calculating the necessary integrals, such as Gaussian Quadrature, but when dealing with complex surfaces there will be many elements and calculating these integrals must be fast and accurate. Hence an alternative method of calculating the integrals was developed which is believed to reduce the computation time.

The diagonal elements H_{ii} and G_{ii} are special cases and there are standard formulae for them (Brebbia [4], Symm [5]). For the off-diagonal elements consider figure 1. Local coordinates are chosen so that the triangle lies on

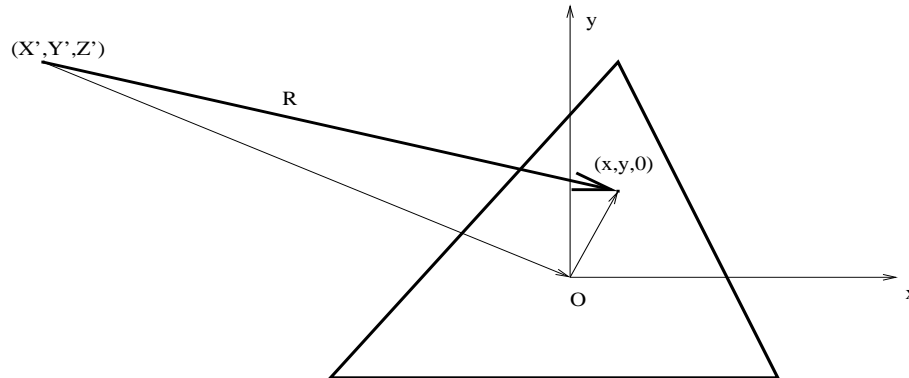


Figure 1: The effect from a node (X', Y', Z') on an element, centroid at the origin

the xy plane, origin at the centroid (since it is always located within the area of the triangle), and base parallel to the x-axis.

R is the distance from point (X', Y', Z') to $(x, y, 0)$ in the triangle. Thus by using a power series in two variables x and y ,

$$\frac{1}{R(X'Y'Z', xyz)} = \sum_{i=0}^{\infty} \frac{1}{i!} \left(x \frac{\partial}{\partial x} + y \frac{\partial}{\partial y} \right)^i \left(\frac{1}{R} \right)$$

which can be expanded about the origin, all derivatives being evaluated at $x = 0$ and $y = 0$.

Doing this, it is possible to express $\frac{1}{R}$ as

$$\frac{1}{R} = \sum_{m,n=0}^{\infty} x^m y^n \Upsilon^{m,n} \quad (2.5)$$

where Υ contains all the constant values, signs, binomials, etc. for ease of computation. In other words Υ only involves the distance from the point (X', Y', Z') to the origin whilst the x and y terms relate to the area of the triangle. Hence the integral of $\frac{1}{R}$ may be written

$$\int \frac{1}{R} ds = \sum_{m,n=0}^{\infty} \left(\int x^m y^n ds \right) \Upsilon^{m,n}. \quad (2.6)$$

Since $\Upsilon^{m,n} \propto R^{-(m+n+1)}$, convergence is ensured if $R > \max(x, y)$. In our implementation we ensure $R > 2 \times \max(x, y)$ and m and n run from 0 to 20.

Here the value of $\int x^m y^n ds$ is known as the m, n -th moment of the element, which can be calculated from figure 2. We introduce variables $X, Y,$

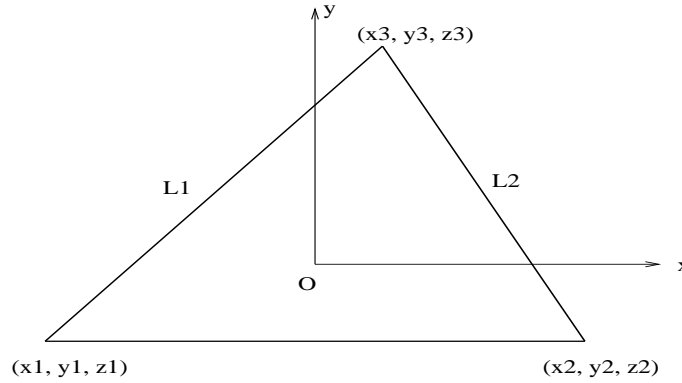


Figure 2: The construction of a triangular element.

and p as follows

- $Y = y3, y1 = y2 = -\frac{Y}{2}$

- $|x_2 - x_1| = 2X$.
- L1 and L2 intercept the x axis at $x = \pm \frac{2}{3}X$.

From this the following can be deduced:-

- L1: $x = py - \frac{2}{3}X$ where p is the tangent of the angle line L1 makes with the y axis,
- $x_3 = pY - \frac{2}{3}X$.
- $x_1 = -p\frac{Y}{2} - \frac{2}{3}X$.
- L2: $x = \left(p - \frac{4X}{3Y}\right)y + \frac{2}{3}X$.
- $x_2 = \frac{4}{3}X - p\frac{Y}{2}$.

Using this information it is possible to create a dimensionless variable which describes uniquely the shape of the triangular element, namely

$$\alpha = \frac{pY}{X}. \quad (2.7)$$

Introducing variables $\zeta = \frac{x}{X}$ and $\eta = \frac{y}{Y}$, L1 and L2 can be written in dimensionless form as

$$L1: \zeta = \alpha\eta - \frac{2}{3}, \quad L2: \zeta = \left(\alpha - \frac{4}{3}\right)\eta + \frac{2}{3}. \quad (2.8)$$

and $ds = XYd\zeta d\eta$. Using the dimensionless forms for L1 and L2, the integration over ζ can be performed to give

$$\int x^m y^n ds = X^{m+1}Y^{n+1} \int_{-\frac{1}{2}}^1 \eta^n \left[\left(\left(\alpha - \frac{4}{3}\right)\eta + \frac{2}{3}\right)^{m+1} \right. \quad (2.9)$$

$$\left. - \left(\alpha\eta - \frac{2}{3}\right)^{m+1} \right] \frac{1}{(m+1)} d\eta$$

$$= X^{m+1}Y^{n+1}M_{m,n}(\alpha) \quad (2.10)$$

where $M_{m,n}(\alpha)$ is a polynomial of degree $m+1$ in α and will be called the normalised moment of the element.

It is possible to show that for these normalised moments

$$\frac{d^n}{d\alpha^n} M_{m+n,0}(\alpha) = \frac{(m+n)!}{m!} M_{m,n}(\alpha). \quad (2.11)$$

Hence if the polynomial $M_{m,0}(\alpha)$ is known for all values of m , simple differentiation will generate the required $M_{m-n,n}(\alpha)$ values.

By setting $n = 0$, the expression for $M_{m,0}(\alpha)$ may be written as

$$M_{m,0}(\alpha) = \int_{-\frac{1}{2}}^1 \sum_{r=0}^m C_r^{(m)}(\eta) \alpha^r d\eta \quad (2.12)$$

where the polynomial coefficients $C_r^{(m)}(\eta)$ depends on m , r , and η . The integration only effects these coefficients so eqn (2.12) may be written as

$$M_{m,0}(\alpha) = \sum_{r=0}^m \alpha^r d_r^{(m)} \text{ where } d_r^{(m)} = \int_{-\frac{1}{2}}^1 C_r^{(m)}(\eta) d\eta. \quad (2.13)$$

For completeness, we write down a compact form for this

$$M_{m,0}(\alpha) = \frac{1}{(m+1)(m+2)} \frac{1}{\alpha(\alpha - \frac{4}{3})} \left[\frac{4}{3} \left(\alpha - \frac{2}{3} \right)^{m+2} + \left(-\frac{1}{2} \right)^{m+2} \left\{ \left(\alpha - \frac{4}{3} \right) \left(\alpha + \frac{4}{3} \right)^{m+2} - \alpha \left(\alpha - \frac{8}{3} \right)^{m+2} \right\} \right]. \quad (2.14)$$

It should be stressed that this form appears to have singularities, but is actually a finite polynomial of degree $m + 1$. The coefficients of α , $d_r^{(m)}$, do not depend on the size nor shape of the triangular elements, therefore they may be calculated once and then referred to whenever an integration is required. Because $M_{m,0}(\alpha)$ is a finite polynomial, it is defined by the coefficients $d_r^{(m)}$ which may be stored in an array and used to obtain exact derivatives of any order for any value of α . This eliminates the requirement to perform time-consuming numerical integrations each time a matrix element is calculated. The required integrations can now be calculated simply by forming a polynomial and then differentiating, i.e.

$$\int \frac{1}{R} ds = \sum_{m,n} \left\{ X^{m+1} Y^{n+1} \frac{m!}{(m+n)!} \frac{d^n}{d\alpha^n} \sum_{r=0}^{m+n} d_r^{(m+n)} \alpha^r \right\} \Upsilon^{m,n}. \quad (2.15)$$

Differentiation with respect to the outward normal of the element, the z-direction in figure 2, will produce the other required integral for the H matrix.

To ensure convergence in the summation eqn (2.5), we test that $\frac{X}{R} < 0.5$ and $\frac{Y}{R} < 0.5$. If not, the triangle is divided into four smaller triangles by joining the midpoints of the three sides. Three of these triangles have exactly the same shape and orientation as the original and therefore have the same reduced moments (Defourny [6]). The central triangle has the same shape but is rotated by 180° , so that its reduced moments are $(-1)^{m+n}$ times the original. In this process, $X \rightarrow \frac{X}{2}$, $Y \rightarrow \frac{Y}{2}$. Further subdivision is performed if the convergence criteria has not yet been achieved. This algorithm is very easily implemented in a computer language which allows recursion.

With the theory behind this new method developed, it was then tested against other methods.

3 The Tetrahedral Example

This method was tested using tetrahedrons to represent the propeller and the hull in an infinite tank of seawater. A schematic of the problem is shown in figure 3. Because of the symmetries in the problem, many of the G and H

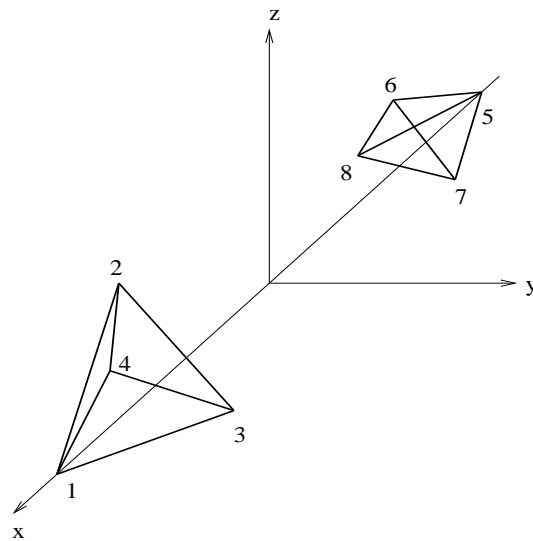


Figure 3: Outline of Tetrahedral Example.

integrals are equal, and there are also identifiable inequalities among them.

To check these equalities and inequalities, the values for the integrals for the off-diagonal elements were calculated via various methods. As well as the method described above, the mathematical package Maple and the accepted numerical method of Gaussian Quadrature were used. The Gaussian Quadrature was performed by a simple ten point Gauss-Legendre integration, which was sufficient for these simple elements to indicate whether the new method was providing satisfactory values (Press *et al.* [7]). The method used by Maple was the Clenshaw-Curtis method.

The three methods do not provide exactly the same values. This is to be expected however since they are all different numerical calculations, and the accuracy of each was different. The Gaussian Quadrature method had a relatively small number of abscissas whilst Maple aimed to achieve a relative error tolerance of approximately 5×10^{-9} , obviously making it the more accurate method of the two. The values of our method were identical to

those provided from Maple to six decimal places. The Gaussian Quadrature method does not match these values for more than two decimal places, but it clearly supports the magnitudes of the other two methods. A quick check of the equalities and inequalities showed that they are all satisfied.

Using this alternative method for calculating the integrals, the matrices H and G were calculated. By selecting suitable boundary conditions which acted as reference values for the calculated electric potentials u , and the negative of the normal component of electric field q , it was possible to solve eqn (2.1) for the unknown u and q values. We have used a point successive over-relaxation method (PSOM) (Janson [8]). This is a method which has been neglected to a certain extent by those seeking to solve large sets of simultaneous equations (Bencham & Lord [9]) but has the great advantage in our particular problem that it allows direct manipulation of individual boundary conditions for the unknowns as it iteratively seeks solutions. Boundary conditions are straightforward on most surfaces but on the hull u and q are related by a highly non linear polarisation relation (Adey *et al.* [10], Zamani & Porter [2]). Starting values of the quantities \mathbf{u} and \mathbf{q} are guessed and then the discrepancy between the i^{th} elements of $H\mathbf{u}$ and $G\mathbf{q}$ is regarded as an indicator of the defects in the values of u_i and q_i : one may write

$$\tilde{u}_i = u_i + \frac{r}{H_{ii}} ((H\mathbf{u})_i - (G\mathbf{q})_i) \quad (3.1)$$

where the old values of \mathbf{u} and \mathbf{q} are used on the right to compute a new value of \tilde{u}_i on the left. Here r is a relaxation factor which may be greater than 1 (over-relaxation) or much less than 1 if a more delicate touch is needed to obtain convergence. As soon as a new value of u_i is calculated, the corresponding q_i can be calculated from the polarisation relation on element i . The procedure is repeated for all i , then iterated until convergence is obtained. It is straightforward to incorporate other conditions onto the elements, i.e. an Impressed Current Cathodic Protection system can easily be modelled where there are anodes attached to the hull which fix the values for u and q at the relevant elements (Zamani & Porter [2]).

4 Calculation of the Electromagnetic Fields

From the above, values for u and q are known for every element on the boundary of the model. All that remains is to calculate the electromagnetic fields due to these potentials and their derivatives at positions within the domain.

While deriving the theory behind the BEM (Brebbia [4]) an equation appears which provides the potential at a point (i, j, k) within the domain,

$$V_{ijk} = \sum_{p=1}^n q_p G_{ijk,p} - \sum_{p=1}^n u_p H_{ijk,p} \quad (4.1)$$

The matrices will need to be recalculated for eqn (4.1) to be used since the point (i, j, k) is not one for which the elements have been previously calculated. Once the potentials have been calculated, the application of numerical differentiation to calculate the negative of the gradient of V at this point provides the electric field. Obviously the number of points at which the potential must be calculated depends on the algorithm used for the numerical differentiation but despite this it is a fairly direct process to calculate the electric field. However to calculate the magnetic field at a point is more difficult.

The accepted method within industry is to mesh the interior of the domain and proceed by calculating \mathbf{E} at each node (Kermorgant [11]). From this the current density can be calculated at each node and then the magnetic field at a point can be calculated by the Biot-Savarts Law which becomes the following summation over the entire volume

$$\mathbf{H} = \frac{1}{4\pi} \sum_V \frac{\mathbf{J} \times \mathbf{R}}{R^3} dV. \quad (4.2)$$

The main drawback of this method is that after having used BEM to restrict the mesh to the boundary to calculate u and q , it is undesirable to now have to mesh the entire volume of the domain. However, all the relations used to arrive at the magnetic field strength are linear which implies that a linear, yet complicated, formula exists which goes straight from the u and q values to \mathbf{H} .

By beginning with the Boit-Savarts Law for \mathbf{H} in terms of the vector potential \mathbf{A} , it can be shown that

$$\mathbf{H} = -\frac{1}{4\pi} \sigma \int_s \frac{u}{R^3} ds \times \mathbf{R} \quad (4.3)$$

where σ is the conductivity of the seawater assumed constant, s is the surface of the domain, and u is the electric potential on the surface (calculated from the BEM). The integral is only over the surface, hence the magnetic field \mathbf{H} at any point within the domain can be calculated numerically by a summation of the contributions from the potentials on each element removing the requirement to mesh the interior of the domain and perform integrations over the volume.

Having developed and tested the procedures described above, it was then implemented on a model of an aircraft carrier with a 50,000 tonne displacement. The boundary was meshed with 5132 triangles. On the model, the hull was coated with a protective paint which was intact, i.e. had high resistance. The effect of this in the real world would be that very little corrosion would occur (Zamani & Porter [2]). Hence there would be very small amounts of current flowing in the sea about the vessel. Hence the expected values of the magnetic field would be extremely small. Since the propeller of the ship does not have a coating, the majority of the sea currents would be focused

on this region meaning that a large peak was expected in the magnetic field about this area.

A plot of the magnitude of the calculated magnetic field at 20m below the base line of the hull is shown in figure 4. Evaluation of the field at this level is standard practice for signature engineers. From the plot it can be

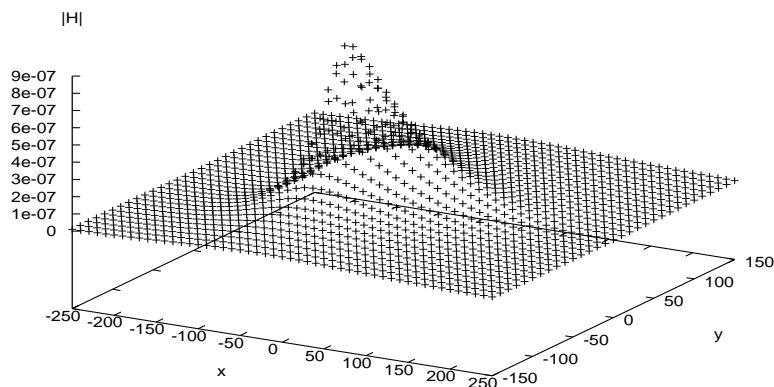


Figure 4: The magnitude of the magnetic field for a ship with a well coated hull at 20m below base line.

seen that the magnitude of the field is indeed very small, and there is a sharp peak in the vicinity of the propeller. The size of the $|\mathbf{H}|$ values is not cause for great concern as it was a direct consequence of the conditions on the hull. Indeed calculations being currently performed indicate that when paint damage is introduced on the hull, the values for the potential on the hull increase as expected and as a direct result the calculated values for $|\mathbf{H}|$ increase to levels which have been experienced in practice.

5 Conclusion and Discussion.

The findings presented here are broadly in agreement with other studies (Zamani & Porter [2]) of the EM signatures of marine vessels due to corrosion. Modelling this physical problem may involve a semi-infinite domain, hence the BEM is the most suitable numerical method for carrying out the analysis. Therefore when the coefficient matrices of the BEM are formed, there will be tens of millions of numerical integrations to be calculated. The

accuracy of the numerical integration is crucial in BEM and can be controlled but in general to perform a reasonably accurate integration numerically takes longer than other processes such as differentiation, and summation. Hence a new method of calculating the integrals was developed which focussed on these issues.

This method involved the meshing of the model using only triangular elements. For the method to work, it was necessary to invest time initially in the calculation of coefficients of a parameter which uniquely described the shape of the triangle. Once these coefficients had been generated and stored, they could simply be referred to whenever an integration was required. The actual integration itself was performed by the summation of a series of derivatives of polynomials which were produced from the stored coefficients and the unique element shape parameter. Hence instead of a numerical integration in the style of Gaussian Quadrature, they were calculated by the more accurate and time efficient processes of differentiation and summation.

The point successive over-relaxation technique is used to solve the sets of equations in the BEM. This had the advantage for the particular problem considered here that it allows polarisation restraints to be imposed at each point as soon as our estimate of u changes.

To compute the magnetic field \mathbf{H} resulting from corrosion currents, we have derived a formula which allows \mathbf{H} to be computed directly from the electric potentials on the boundaries. This has the great advantage that it does not require intermediate values of electric potential, electric field and current to be calculated throughout the volume with a subsequent volume integration of the Biot-Savarts Law to find \mathbf{H} , but computes \mathbf{H} directly from the output from the BEM.

More details of the methods described in this paper and additional results may be found in a thesis by one of the authors (Allan [12]).

6 Acknowledgements

One of us, P. Allan, is grateful for the financial support from PPARC and BAE Systems.

References

- [1] Jeffery, I. & Brooking, B., *A Survey of New Electromagnetic Stealth Technologies*, www1.davis-eng.com/docs/New_Electromagnetic_Stealth.pdf
- [2] Zamani, N.G., & Porter, J.F., Boundary Element Simulation of the Cathodic Protection System in the Destroyer Class 280. *Boundary Element Techniques: Applications in Fluid Flow and Computation Aspects*, eds. C.A. Brebbia & W.S. Venturini, Computational Mechanics Publications, pp. 123-138, 1987.

- [3] Wang, Y., Brennan, D.P., Porter, J.F. & Karisallen, K.J., Evaluation of a Shipboard ICCP System using Boundary Element Code. *2nd International Warship Cathodic Protection Symposium*, Cranfield University, 2003.
- [4] Brebbia, C.A., *The Boundary Element Method for Engineers*, Pentach Press, 1978.
- [5] Symm, G.T., An Introduction to the Application of Boundary Element Methods in Electrostatics. *BETECH 86 - Proceedings of the 2nd Boundary Element Technology Conference*, eds. J.J. Connor & C.A. Brebbia, Computational Mechanics Publications, pp. 63-75, 1986.
- [6] Defouny, M., The Boundary Element Method Applied to Electric Field Computation: Generation, Computation and Results with Examples in the High Voltage Field. *BETECH 86 - Proceedings of the 2nd Boundary Element Technology Conference*, eds. J.J. Connor & C.A. Brebbia, Computational Mechanics Publications, pp 75-84, 1986.
- [7] Press, W.H., Flannery, B.P., Teubolsky, S.A. & Vetterling, W.T., *Numerical Recipes in C: The Art of Scientific Computing*, Cambridge University Press, 1988.
- [8] Jansson, P.A., *Deconvolution of Images and Spectra (Second Edition)*, Academic Press, 1997.
- [9] Bencham, S.P. & Lord, J.A., *EMMA_FFMM3D. Theory and Initial Results from a Multi-Level Fast Multi-pole Code*, BAe Systems Advanced Technology Centre (Sowerby) (Confidential in Commerce).
- [10] Adey, R.A., Brebbia, C.A. & Niku, S.M., BEASY-CP - A System for Analysis of Galvanic Corrosion and Cathodic Protection using Boundary Elements. *BETECH 86 - Proceedings of the 2nd Boundary Element Technology Conference*, eds. J.J. Connor & C.A. Brebbia, Computational Mechanics Publications, pp. 85-108, 1986.
- [11] Kermorgant, H., Modelling and Characterization of the Underwater Electromagnetic Field Radiated by an UUV in the Static Domain. *MARELEC '99 - 2nd International Conference on Marine Electromagnetics*, pp. 459-469, 1999.
- [12] Allan, P.J., *Ph. D Thesis, A Study of the Electromagnetic Signatures of Marine Vessels using the Boundary Element Method*, University of Glasgow, 2004.